Liquid Crystals
Publication details, including instructions for authors and subscription information:
http://www.informaworld.com/smpp/title~content=t713926090

Cubic phases of binary systems of 4'-*n*-tetradecyloxy-3'-nitrobiphenyl-4-carboxylic acid (ANBC-14)-*n*-alkane

Shoichi Kutsumizu; Koushi Morita; Shinichi Yano; Shuichi Nojima

Online publication date: 11 November 2010

To cite this Article Kutsumizu, Shoichi , Morita, Koushi , Yano, Shinichi and Nojima, Shuichi(2002) 'Cubic phases of binary systems of 4'-*n*-tetradecyloxy-3'-nitrobiphenyl-4-carboxylic acid (ANBC-14)-*n*-alkane', Liquid Crystals, 29: 11, 1459 — 1468
To link to this Article: DOI: 10.1080/02678290260372655
URL: http://dx.doi.org/10.1080/02678290260372655

LIQUID CRYSTALS, 2002, VOL. 29, NO. 11, 1459–1468

Taylor & Francis
Taylor & Francis Group

Cubic phases of binary systems of 4′-*n*-tetradecyloxy-3′-nitrobiphenyl-4-carboxylic acid (ANBC-14)–*n*-alkane

SHOICHI KUTSUMIZU*, KOUSHI MORITA, SHINICHI YANO
Department of Chemistry, Faculty of Engineering, Gifu University, 1-1 Yanagido, Gifu 501-1193, Japan

and SHUICHI NOJIMA
School of Materials Science, Japan Advanced Institute of Science and Technology (JAIST), 1-1 Asahidai, Tatsunokuchi, Nomi, Ishikawa 923-1292, Japan;
Graduate School of Science and Engineering, Tokyo Institute of Technology, 2-12-2 O-okayama, Meguro-ku, Tokyo, 152-8552, Japan

(*Received 30 April 2002; accepted 17 June 2002*)

The phase behaviour of the binary systems 4′-*n*-tetradecyloxy-3′-nitrobiphenyl-4-carboxylic acid (ANBC-14)–*n*-alkane (*n*-tetradecane or *n*-hexadecane) was investigated by differential scanning calorimetry, polarizing optical microscopy, and X-ray diffraction. The phase behaviour was a function of temperature (T) and the effective carbon number of the system (n^*), where n^* involves carbon atoms both from the alkoxy group of ANBC-14 and from the *n*-alkane added. ANBC-14 shows no cubic phase, but the addition of *n*-alkane induced cubic phases when $n^* \geqq c.\ 15$. An interesting point is that the type of cubic phase is $Ia3d$ for $15 \leqq n^* \leqq 17$, while an $Im3m$ type is formed for $18 \leqq n^* \leqq 20$. Furthermore, for $n^* = 22$, two types of cubic phase, one with $Im3m$ symmetry in the low temperature region and the other with $Ia3d$ in the high temperature region, were observed both on heating and cooling. The phase diagram with respect to T and n^* is very similar to that of pure one-component ANBC-*n*, which is a function of T and the number of carbon atoms in the alkoxy group *n*.

1. Introduction

Thermotropic cubic liquid crystalline phases have been attracting much attention recently and many types of compound exhibiting thermotropic cubic phases have been synthesized and characterized [1–3]. Among them, one of the most famous classes of compound is probably the 4′-*n*-alkoxy-3′-nitrobiphenyl-4-carboxylic acids, designed as ANBC-*n*, where *n* is the number of carbon atoms in the alkoxy group. These compounds were first synthesized by Gray and co-workers in 1957 [4] and the $n = 16$ and $n = 18$ homologues have long been known to exhibit thermotropic cubic phases, initially called the smectic D phase [5, 6], later D [7, 8], cubic D, or simply cubic (Cub) phase [3]. The molecular structure is very simple, having a biphenyl core with a long alkoxy chain at the 4′-position, a hydrogen-bonding carboxylic acid group at the 4-position, and at the side, in the 3′-position, a nitro group of large dipole moment. Roughly speaking, the molecular shape is rod-like. Such optically anisotropic rod-like molecules form an optically isotropic cubic organization in a certain temperature range [5, 6, 9, 10], neighboured by other optically anisotropic phases with lamellar structures such as smectic C and A (SmC and SmA) phases, or the isotropic liquid (I) phase, when $n \geqq 15$, and the temperature region widens monotonously with increasing n [10]. Thus, it is clear that the number of carbon atoms in the alkoxy group n is a key factor for forming the Cub phase, and lengthening the alkoxy tail stabilizes the Cub phase(s).

The structure of the Cub phase for $n = 16$ was identified as being of the space group $Ia3d$, and reasonably assumed to be a bicontinuous type [7], by analogy with the structure of a lyotropic cubic phase (labelled Q phase) first postulated by Luzzati and co-workers, where rod-like micelles are joined 3-by-3 to form two sets of interwoven networks (a skeletal graph) [11]. It is generally considered that the aromatic core part forms the 'skeletons' in the skeletal graph and the alkyl chains fill the remaining space between the skeletons [11], but this picture is not so certain for the bicontinuous structure

* Author for correspondence; e-mail: kutsu@cc.gifu-u.ac.jp

Liquid Crystals ISSN 0267-8292 print/ISSN 1366-5855 online © 2002 Taylor & Francis Ltd
http://www.tandf.co.uk/journals
DOI: 10.1080/0267829021000026078

itself, and the reverse picture, i.e. with the methyl end groups of the chains on the skeletons, may be possible [12].

Saito, Sorai, and their co-workers paid attention to the role of the alkoxy chains in the Cub phase(s) of ANBC-n homologues, and investigated the phase diagrams of binary systems of ANBC-n having $n = 8$, 16 and 18 with n-tetradecane [13]. One of their important results is that the phase diagram of the binary system ANBC-16 (or ANBC-18)–n-tetradecane is quite similar to the diagram of the neat one-component ANBC-n system, and the result is reasonably understood in terms of the effective carbon number n^* (or n_C in [13]) that involves carbon atoms both from the alkoxy group of ANBC-16 (or ANBC-18) and from the n-tetradecane; n^* is the apparent carbon number per ANBC-n biphenyl core in the system and shown as $n^* = n + 14\,[x/(1-x)]$, where n is the number of carbon atoms in the alkoxy group of ANBC-n ($n = 16$ or 18, in this case), '14' is the number of carbon atoms in n-tetradecane, and $x (0 \leqq x \leqq 1)$ is the molar fraction of n-tetradecane in the system. The result demonstrates that the role of the top part of the alkoxy chain in neat ANBC-n systems acts as a solvent, just like the solvent in the lyotropic Cub phases of lipid–solvent systems. On the other hand, the phase diagram of the ANBC-8–n-tetradecane binary system showed no Cub phase region, from which they concluded that the *effective* core size required for exhibiting the Cub phase is larger than the size of a dimerized biphenyl core plus two C_8 alkyl tails at the ends. They extended their idea to other compounds exhibiting Cub phases and confirmed the importance of the effective number of paraffinic carbon atoms for the appearance of Cub phases, irrespective of the molecular structure and/or intermolecular interactions [14].

Very recently, we have constructed the phase diagram for the pure one-component ANBC-n, unequivocally establishing the phase type of the Cub phase region, as shown in figure 1 [15, 16]. Unexpectedly and surprisingly, the Cub region that had been assumed to contain a single phase was found to contain two types of Cub phase, one with $Im3m$ symmetry (and denoted as Cub I in this paper) and the other with $Ia3d$ symmetry (Cub II); the type of cubic phase was $Ia3d$ for $15 \leqq n \leqq 18$, in agreement with previous reports for $n = 16$ [7] and 18 [17, 18], while an $Im3m$ type was found for $19 \leqq n \leqq 21$, both on heating and cooling. A complicated feature of the Cub phase region is that the $Im3m$ Cub phase region lies between two regions of the $Ia3d$ Cub phase, the $Ia3d$ type being again observed in the high temperature region for the $n = 22$ and 26 homologues, with a cubic-to-cubic phase transition in the mid temperature range of the Cub region on heating, whereas only the $Ia3d$ type is observed on cooling [15, 16, 19, 29]. Since the dependence of the Cub phase type on n in pure one-component ANBC-n systems is not simple, the question arises again as to whether the top part of the alkoxy chain in ANBC-n is really liquid-like, free from conformational restriction, as stated by Saito *et al.*, when filling the aliphatic subspace of the Cub phase(s).

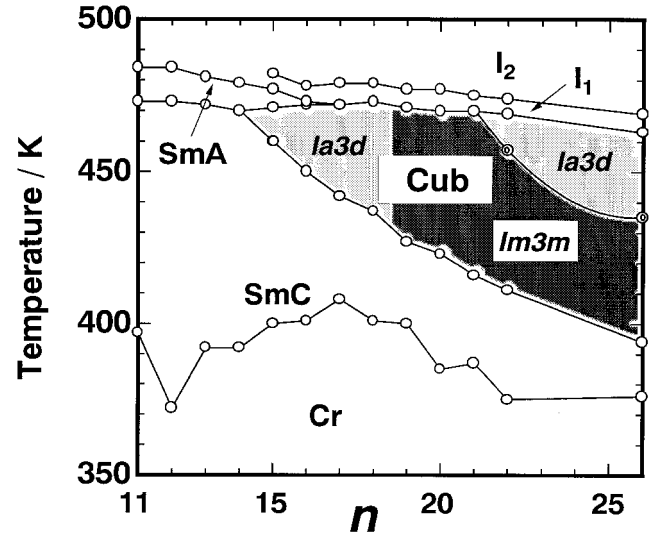

Figure 1. Phase diagram for ANBC-n on heating (Cr, crystal; SmC/A, smectic C/A; Cub, cubic; I_1, I_2, isotropic liquid phases). The space group of the Cub phases determined by XRD is also shown. Reprinted from [16] with permission from Taylor & Francis.

In this paper, we have extended the work by Saito and co-workers and examined the phase behaviour of binary systems of the $n = 14$ homologue (ANBC-14) and n-alkane (n-tetradecane or n-hexadecane) by differential scanning calorimetry (DSC), polarizing optical microscopy (POM), and X-ray diffraction (XRD). We chose ANBC-14 as the ANBC-n component, with an alkoxy chain 1 carbon atom shorter than the alkoxy chain length required for the Cub phase(s) in ANBC-n homologues and therefore exhibiting *no* Cub phase. If the top of the alkoxy tail really acts as a solvent, in other words acts as a continuum, the top part, being connected to the ANBC-n biphenyl core, would not be necessary and the addition of n-alkane to ANBC-14 would induce the formation of the Cub phase(s). Furthermore, we also focused attention on the phase type in the Cub region of the binary systems, and examined to what extent the effective carbon number n^* of the systems influences and determines the formation of different types of Cub phase.

2. Experimental

2.1. *Preparation*

ANBC-14 was prepared according to the method of Gray *et al.* [4, 21]. The sample was recrystallized from ethanol several times and confirmed to be fully pure by

infrared (IR), ^{1}H NMR, mass spectroscopy (MS), thin layer chromatography, DSC, and elemental analysis. The phase transition temperatures obtained were in excellent agreement with previous reports [10].

n-Tetradecane (m.p. 6°C; b.p. 252°C) and *n*-hexadecane (m.p. 18°C; b.p. 287°C) were from Nacalai Tesque (purity >99%) and used as received. Binary mixtures of ANBC-14 with *n*-tetradecane/*n*-hexadecane were prepared in the present study by simple mixing in the isotropic liquid state as detailed below.

2.2. *Measurements*

IR spectra were recorded using a Perkin-Elmer 1640 and a Perkin-Elmer system 2000 Fourier transform IR spectrometer. ^{1}H NMR and MS spectra were recorded using a JEOL JNM-α400 spectrometer and a Shimadzu GCMS QP-1000 system, respectively.

The phase transitions were examined with a Seiko Denshi DSC-210 interfaced to a TA data station (SSC 5000 system). The measurements were performed using a dry N_2 flow of *c.* 40 ml min^{-1} and at a heating/cooling rate of 5 K min^{-1}. Weighed binary samples were hermetically sealed into an Al pan (types 560-001 and 560-002 for liquid samples) and kept at 488 K in the isotropic liquid state for 15 min to mix the two components fully, followed by cooling to 303 K at 5 K min^{-1}; samples were then ready for measurements. Recording was therefore started from the second heating run and the repeated scans for the same samples between 303 and 503 K gave perfect reproducibility, indicating no loss of the *n*-alkane.

The texture of each mesophase was observed using a Nikon Optiphot-pol XTP-11 polarizing optical microscope equipped with a Mettler FP82 hot stage and a Mettler FP80 central processor at a heating/cooling rate of 5 K min^{-1}. For the POM observations, binary samples were packed into an Al pan, covered with a cover glass, and sealed with an epoxy adhesive agent (Araldite Rapid®, Vantico). Then, the samples were heated to and kept at 488 K for 15 min to mix the two components fully. The samples were then removed from the Al pan and sandwiched between two cover glasses, whose four edges were hermetically sealed with an epoxy adhesive agent to avoid the loss of the alkane component during observations at elevated temperatures.

For XRD measurements at elevated temperatures, binary samples were prepared as for the samples for POM observation, and then sandwiched between a 0.06–0.08 mm thick cover glass (Matsunami Glass, thickness No. 00) and a 0.25 mm thick PET sheet with a 0.5 mm Teflon spacer, sealed with an epoxy adhesive agent. The samples, covered with an Al foil with windows, were placed in a Mettler FP82HT hot stage, and the temperature was controlled within ±0.1°C by the Mettler FP90 central processor. The accuracy of the temperature was checked using a calibrated Fe–constantan thermocouple. For recording the XRD patterns, a MAC Science X-ray generator (M18XHF) was operated with a copper target at 40 kV and 30 mA, and the Cu Kα radiation ($\lambda = 0.154$ nm) was point-focused with Huxley–Holms optics. The scattered X-rays were detected by a one-dimensional proportional counter (PSPC) with an effective length of 10 cm. The distance between the sample and PSPC was about 40 cm; the geometry was further checked by using chicken tendon collagen, which gives a set of sharp diffractions corresponding to a spacing of 65.3 nm, and α-stearic acid, giving a set of diffractions at 3.95 nm. The accumulation time for each measurement was 500–3 600 s, depending on the intensity obtained and the quality needed.

3. Results and discussion

Figure 2 shows the DSC traces of the ANBC-14–*n*-tetradecane binary system on the second heating run, where n^* is the effective carbon number of the system, given by $n^* = 14 + 14\,[x/(1-x)]$ with x being the molar fraction of *n*-tetradecane, as mentioned in the Introduction.

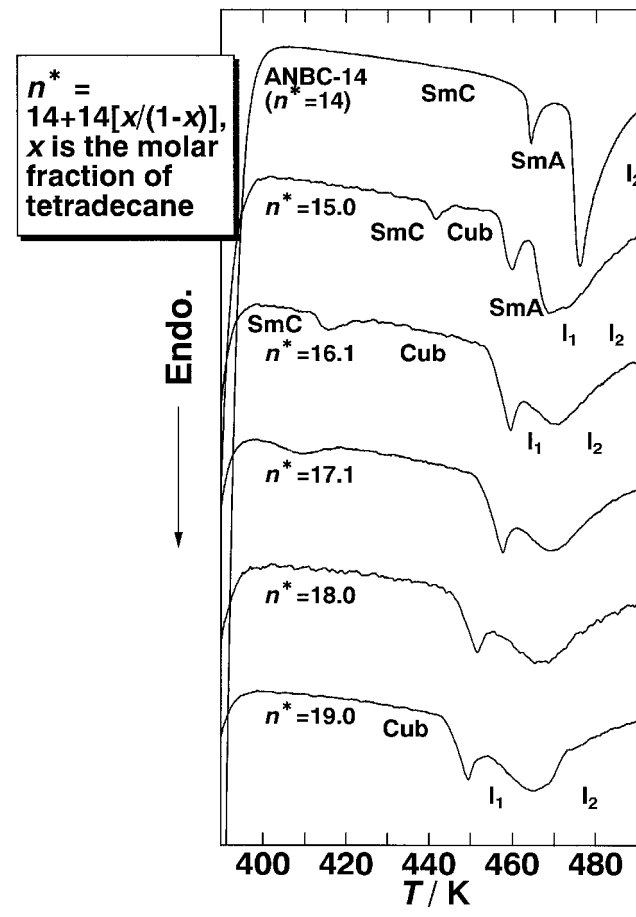

Figure 2. DSC traces of the ANBC–*n*-tetradecane binary system on the second heating run. The amount of *n*-tetradecane in the system is designated by the effective carbon number n^* (see text).

ANBC-14 shows two kinds of lamellar mesophases, a smectic C (SmC) phase (390–465 K) and a smectic A (SmA) phase (465–476 K), and no cubic (Cub) phase. As n-tetradecane was added as the second component and thus n^* was increased from 14, another phase appeared around 450 K. This phase was identified as a Cub phase by POM observations which showed, on heating, the appearance and growth of completely black areas with straight edges in the SmC schlieren texture between crossed polarizers [5]. The 'textures' taken for $n^* = 16.1$ and 18.9 at the phase transition are shown in figure 3. As n^* was increased, the SmC–Cub phase transition temperature was lowered and became obscure, and concomitantly, a broad hump around 470 K became obvious, which was not apparent for ANBC-14. Such humps are seen at 470–480 K for ANBC-n homologues with $n \geqq 15$ [10], and assigned to a structured liquid (I_1)–normal isotropic liquid (I_2) phase transition [10].

An interesting fact was seen for $n^* = 15.0$. On the second heating (the first scan of the measurements, see Experimental section), the Cub and SmA phases were observed at 441.9–459.8 K and at 459.8–468.8 K, respectively; but on the third heating after cooling from 503 to 303 K, the Cub phase region was narrowed (447.2–456.3), eroded by the SmA phase region (456.3–468.5 K). Finally the Cub phase disappeared on the fourth heating. Such an instability of the Cub phase was also observed for ANBC-15 [22], and is supposed to be closely connected with the fact that the aliphatic content of $n = 15$ or $n^* = 15$ is a minimum for forming the Cu phase(s) in ANBC-n homologues and related systems.

The n^* dependence of the phase transitions is summarized in figure 4. The SmA phase region vanishes around $n^* = 16$, being replaced by the I_1 phase region from the high temperature side. The Cub–SmA/I_1 and I_1–I_2 phase transition temperatures are almost independent of n^*, whereas the SmC–Cub transition temperature is lowered almost linearly with n^*. These features are also seen in the phase diagram of the pure one-component ANBC-n system as a function of temperature and n (figure 1). It should be noted that the phase diagram of ANBC-n is reproduced by adding the aliphatic component (n-tetradecane) to ANBC-14 that itself shows no Cub phase.

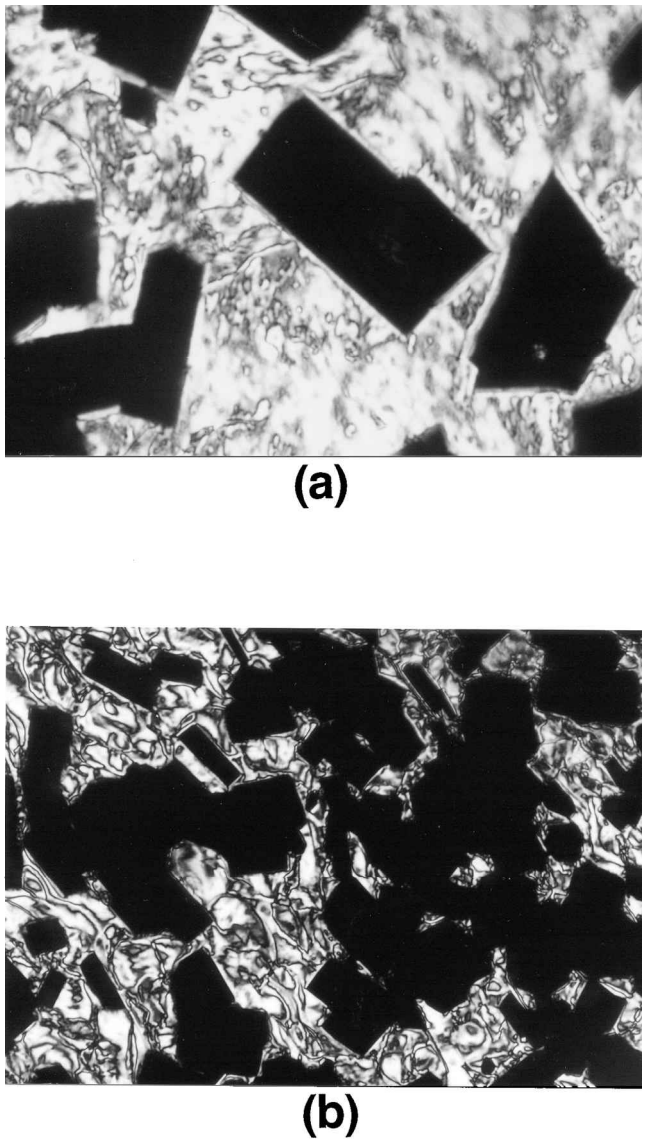

Figure 3. Polarizing photomicrographs near the SmC–Cub phase transition for the ANBC-14–n-tetradecane system on the second heating run: (a) at 427.4 K for $n^* = 16.1$ and (b) at 396.7 K for $n^* = 18.9$.

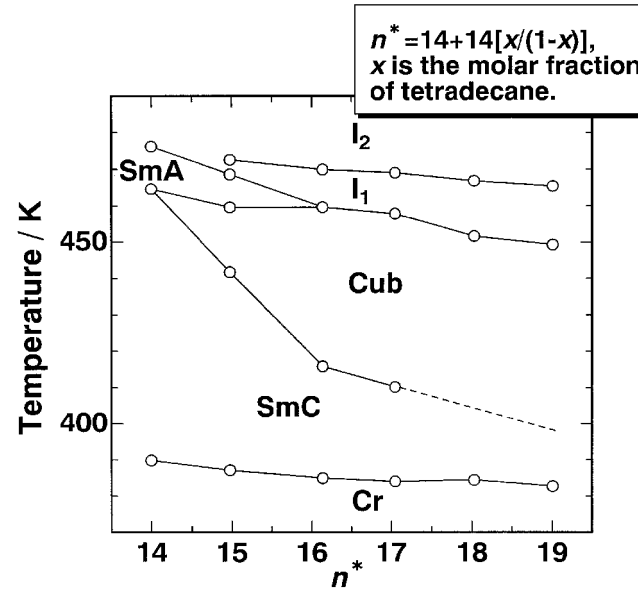

Figure 4. Plots of the phase transition temperatures versus n^* for the ANBC–n-tetradecane binary system on the second heating run.

As mentioned above, the SmC–Cub phase transition was obscure by DSC above $n^* > 17$, as indicated by a broken line in figure 4. The transition interval for $n^* = 17.1$ was significantly broader compared with the case of $n^* = 16.1$ or 15.0 and probably superposed on the tail of the large low temperature endothermic peak assigned to the Cr–SmC transition (around 385 K); the high content of the second component ($x > 0.2$) would widen the heterogeneous region at the Cr–SmC and SmC–Cub transition intervals.

Figure 5 shows the DSC traces of the ANBC-14–n-hexadecane binary system on the second heating run, where n^* is given by $n^* = 14 + 16\ [x/(1-x)]$ with x being the molar fraction of n-hexadecane in the system. The addition of the aliphatic component, n-hexadecane, induced a Cub phase at and above $n^* = 15.1$, and the SmA phase region disappeared above $n^* = 15.4$. These two features are in good agreement with those in the phase diagram for ANBC-n; the Cub phase is formed for $n \geqq 15$ and the temperature interval of the SmA phase is about 1 K for $n = 16$ and the phase disappears for $n \geqq 17$ (see figure 1). Unlike the ANBC-14–n-tetradecane system shown in figure 2, the SmC–Cub phase transition peak was detected by DSC even for $n^* = 21.7$, but the transition enthalpy rapidly decreased around $n^* = 17$, being as low as 0.2 J g^{-1} (corresponding to 0.1 kJ mol^{-1}). The temperature scale is shifted by 15–25 K to the low temperature side compared with the diagram for ANBC-n due to the freezing point depression effect.

The phase type for the Cub region was examined by XRD and selected patterns are presented in figure 6. Here, $q = (4\pi/\lambda)\sin\theta$, $\lambda = 0.154$ nm, and $\theta =$ scattering angle. The existence of two types of Cub phases was confirmed. As seen in (*a*), (*d*) and (*f*), one type of pattern exhibits two strong peaks with the ratios of the reciprocal spacings being $\sqrt{3} : \sqrt{4}$ and sometimes has a few very weak peaks with the ratios $\sqrt{8} : \sqrt{10}$. This type of pattern is characteristic of the most commonly observed Cub phase with space group $Ia3d$, and the peaks are probably indexed as $\sqrt{6} : \sqrt{8} : \sqrt{16} : \sqrt{20}$; the indices are doubled, although this is not mathematically driven because in most cases we could not detect the peak corresponding to the ratio of $\sqrt{14}$. The fact that some homologues of pure one-component ANBC-n also exhibit an $Ia3d$ type Cub phase inclined us to this assignment. Thus, the whole Cub temperature regions of $n^* = 16.0$ in (*a*), 17.1

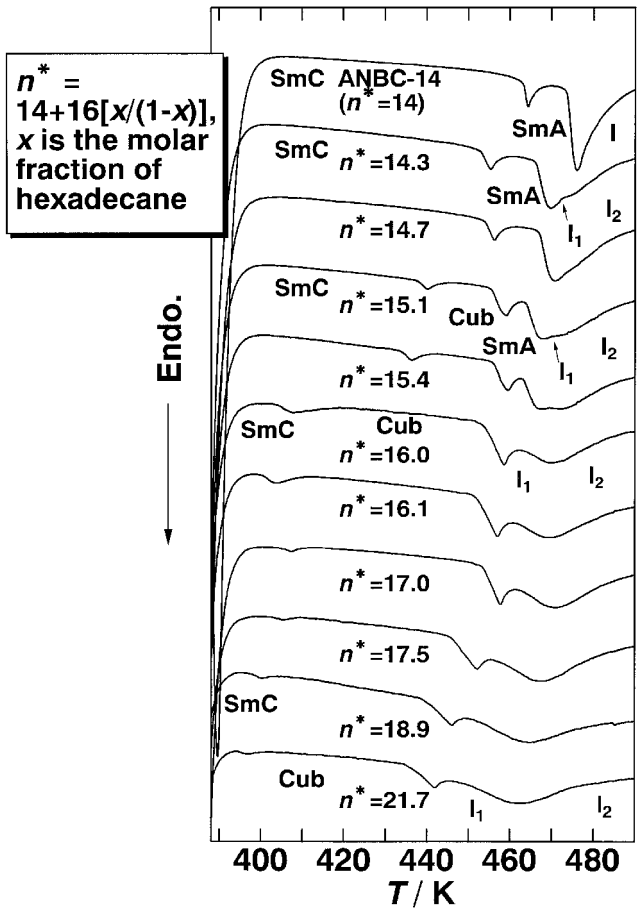

Figure 5. DSC traces of the ANBC-14–n-hexadecane binary system on the second heating run, where n^* is the effective carbon number of the system.

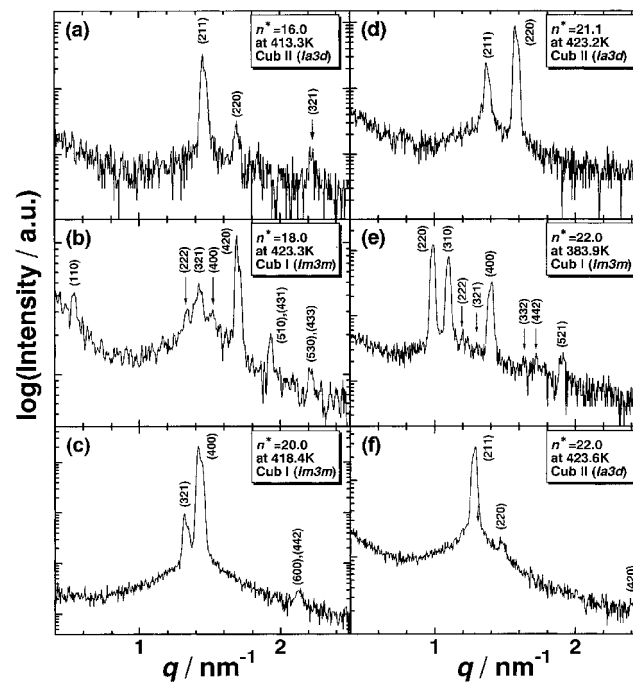

Figure 6. XRD patterns at temperatures in the Cub phase region for the ANBC-14–n-hexadecane system with various n^*: (*a*) at 413.3 K for $n^* = 16.0$, (*b*) at 423.3 K for $n^* = 18.0$, (*c*) at 418.4 K for $n^* = 20.0$, (*d*) at 423.2 K for $n^* = 21.1$, (*e*) at 383.9 K for $n^* = 22.0$ and (*f*) at 423.6 K for $n^* = 22.0$. In each figure, Miller indices and the Cub phase type determined are shown.

(not shown here) and 21.1 in (*d*) and the high temperature region of $n^* = 22.0$ are identified as having space group $Ia3d$.

Another type of pattern is seen in (*b*), (*c*) and (*e*). In this case, the indices of the peaks observed should be doubled because the ratios $\sqrt{7}$ and $\sqrt{15}$ are not compatible with any Cub phases; thus, the phase is identified as a body-centred Cub phase from among the 6 space groups $I23$, $I2_13$, $Im3$, $I432$, $I43m$ and $Im3m$, most probably $Im3m$, the most symmetrical type. Hence, the entire Cub temperature regions of $n^* = 18.0$ in (*b*), 19.1 (not shown here) and 20.0 in (*c*) and the low temperature region of $n^* = 22.0$ are identified as having space group $Im3m$.

The phase diagram within the Cub 'phase' region of the ANBC-14–*n*-hexadecane system is shown in figure 7, where transition temperatures, full circles, were determined by DSC and POM, and the phase types of the Cub phases were determined by XRD, as mentioned above. Three important points should be noted.

(1) Compared with the diagram shown in figure 2, the addition of *n*-hexadecane to ANBC-14 gave almost the same effect as that by *n*-tetradecane; the Cub phase region is induced above around $n^* = 15$, and concomitantly, the SmA phase region disappeared above $n^* = 16$, being replaced by the I_1 phase region. The difference in the carbon number between *n*-tetradecane and *n*-hexadecane being two gave no difference in the binary phase diagram. This fact implies that both *n*-tetradecane and *n*-hexadecane simply act as an aliphatic component (at least in the Cub region); in other words, they act as a solvent as in the lyotropic Cub phases in lipid–solvent systems, as already pointed out by Saito and co-workers [13].

(2) The binary system of ANBC-14 with an aliphatic component exhibits two types of Cub phase, one with space group $Im3m$ and the other with $Ia3d$, which is very similar to the phase diagram for pure one-component ANBC-*n* (figure 1); the $Ia3d$ type is seen for $15 \leqq n^* \leqq 17$ and the $Im3m$ type for $18 \leqq n^* \leqq 21$, fairly in agreement with the diagram for ANBC-*n* with the $Ia3d$ type for $15 \leqq n \leqq 18$ and the $Im3m$ type for $19 \leqq n^* \leqq 21$ [15, 16].

(3) The mixture of $n^* = 22$ exhibits two types of Cub phase successively on heating, which is also similar to the cases of ANBC-22 and -26 [19, 20].

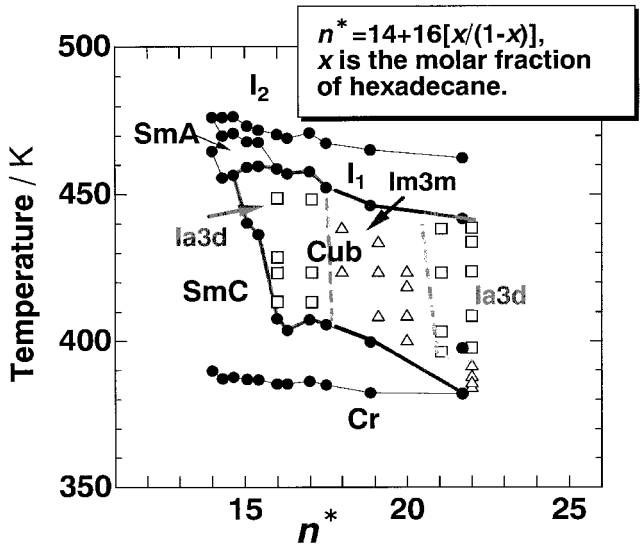

Figure 7. Phase diagram of the ANBC-14–*n*-hexadecane system as a function of temperature (on heating) and n^*: phase transition temperatures (full circles) were determined by DSC and POM, and the space groups of the Cub phase (open triangles, $Im3m$; open squares, $Ia3d$) were determined by XRD.

Points (2) and (3) give rise to an important conclusion from the present study, namely that the effective carbon number n^*, instead of the alkoxy chain length n of ANBC-*n*, determines the type of Cub phase formed in the binary system, and therefore, the complicated phase diagram within the Cub region for ANBC-*n* is not a special case, but is a general feature such as may also be seen in some lyotropic Cub systems. In other words, the formation of the Cub phases and the *phase type* stabilized in ANBC-*n* can be understood by considering the presence of two competing parts, the flexible and hydrophobic aliphatic tails vs the rigid and partly hydrophilic ANBC-*n* aromatic core (containing a hydrogen-bonded COOH linkage). Regarding the reappearance of the $Ia3d$ Cub II phase at higher n or n^*, however, it is probable that weakening of the hydrogen-bonded COOH linkage in the core part plays an important role, as is discussed in our preceding paper [16].

Figure 8 presents the plots of *d*-spacing versus temperature for the ANBC-14–*n*-hexadecane systems with $n^* = 16.0$, 20.0 and 22.0. Open symbols represent the data on heating, and for $n^* = 20.0$ and 22.0, a few data on cooling are included as filled symbols. Three points are noted:

(1) For $n^* = 16.0$ in (*a*), the variation of the SmC layer spacing with T is roughly linear and seems continuous with the temperature variation of the $Ia3d$ Cub II (2 1 1) spacing across the phase boundary, suggesting the existence of an epitaxial relationship between the two phases. A similar result was seen for ANBC-16 [16], and more generally for lyotropic cubic systems at the lamellar to $Ia3d$

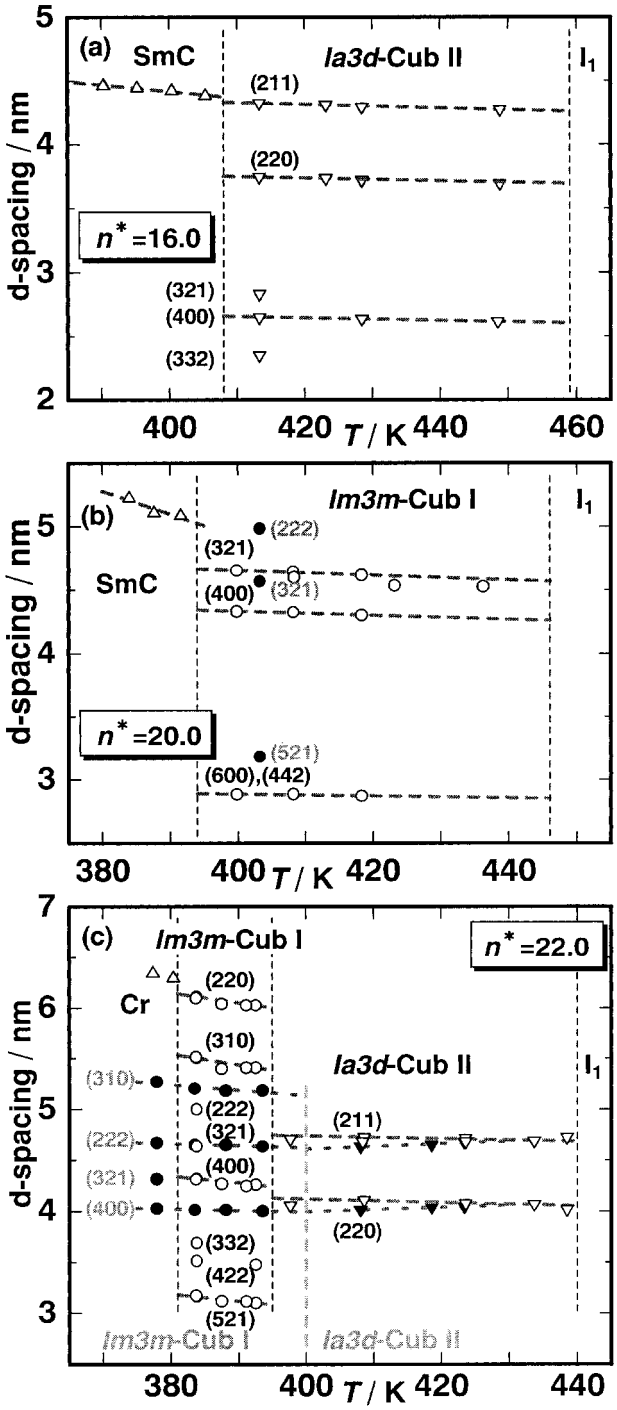

Figure 8. Plots of d-spacing versus temperature T for the ANBC-14–n-hexadecane system with (a) $n^* = 16.0$, (b) $n^* = 20.0$ and (c) $n^* = 22.0$, during heating (open symbols, black labelling) and cooling (filled symbols, grey labelling).

Cub phase transition [23]. On the other hand, for $n^* = 20.0$ in (b), there is a small discontinuity between the SmC and the $Im3m$ Cub I (3 2 1) spacings on heating, and the SmC layer spacing rather seems to change continuously into the Cub I (2 2 2) spacing, although we could not detect the Cub I (2 2 2) reflection on heating. In the $Im3m$ Cub I phases in ANBC-n, not the (2 2 2) plane, but the (3 2 1) plane is the highest density plane [16, 18–20], and probably the same is true for the binary system, although sometimes other planes were most intensely observed as seen in figure 6(c). Related to this, in a mixture of ANBC-18 with 3,5-didodecyloxybenzoic acid, the $Im3m$ Cub I phase was induced at 35% of the second component, where the (3 2 1) reflection was most intensely observed [24]. For $n^* = 22.0$ in (c), the SmC layer spacing changes to the $Im3m$ Cub I (3 2 1) spacing and then to the $Ia3d$ Cub II (2 1 1) spacing with discontinuities at the phase transitions on heating.

(2) As clearly seen from (a), (b) and (c), the slopes of the d versus T plots are all slightly negative on heating in the Cub temperature region, as is usually seen for thermotropic Cub phases. Assuming that the Cub phases were regarded as crystals, the apparent thermal volume expansion coefficients α were estimated by using the relation $\alpha = (1/a^3)(\partial a^3/\partial T)$, where a is the cubic lattice constant. The results were: -1.0×10^{-3} K^{-1}, -1.4×10^{-3} K^{-1}, -1.0×10^{-3} K^{-1}, -1.3×10^{-3} K^{-1}, -1.0×10^{-3} K^{-1} and -1.1×10^{-3} K^{-1} for $n^* = 16.0$, 17.1, 18.0, 19.1, 20.0 and 21.1, respectively; and for $n^* = 22.0$, -4.1×10^{-3} K^{-1} in the low temperature Cub I phase region, and -2×10^{-4} K^{-1} in the high temperature Cub II phase region. Almost the same values were obtained for pure one component ANBC-n [16]. Note that the negative value of α estimated in this way does not imply a negative thermal expansion of the system, but that the number of molecules contained in the Cub unit lattice actually decreases with increasing temperature.

(3) Reversibility: For $n^* = 20.0$ in (b), both heating and cooling runs showed the $Im3m$ Cub I phase, and the lattice parameters on heating and cooling were almost identical, similarly to the case of ANBC-20 [16]. The situation is, however, different for $n^* = 22.0$ shown in (c). As mentioned in the Introduction, in the corresponding one-component system, ANBC-22, exhibits $Im3m$ Cub I and $Ia3d$ Cub II phases on heating, whereas only the $Ia3d$ Cub II phase is formed on cooling [16]. By contrast, the $n^* = 22.0$ binary mixture showed $Im3m$ Cub I and $Ia3d$ Cub II phases both on heating and cooling; the Cub I–Cub II phase transition is thermally reversible in the $n^* = 22.0$

mixture. The transition temperature was around 390 K on heating and on cooling around 400 K, at a slightly higher temperature. This result was reproducible for duplicate measurements, although we could not find any clear answer as to why the transition occurs at a higher temperature on cooling. The apparent thermal volume expansion coefficient α of the Cub I phase, as estimated in (2) above, was $-1.4\times10^{-3}\ K^{-1}$, negative with temperature, but the α value of the Cub II region was positive ($1.6\times10^{-3}\ K^{-1}$). Furthermore, the Cub I lattice parameter on cooling was significantly (6%) smaller than the parameter on heating, although the same lattice parameter was obtained for the Cub II phase both on heating and cooling. A probable reason for these differences for $n^*=22.0$ is a micro-segregation between ANBC-14 and n-hexadecane, and this process may occur at low temperatures when the amount of the second component is relatively high.

Figure 9 shows the comparison between the n^* dependence of the Cub lattice parameter (a) in the ANBC-14–n-hexadecane system (full circles) and the corresponding n dependence for ANBC-n (open circles). The data for ANBC-n are cited from [16], and all data plotted are summarized in the table. For the $Ia3d$ Cub II phase in the ANBC-14–n-hexadecane system, the a value increases almost linearly with n^*, with a relation of $a=8.28+0.14n^*$ (correlation coefficient $r=0.997$), whereas for ANBC-n, the dependence of a on n is roughly given by $a=7.80+0.18n$ ($r=0.86$); the r value for ANBC-n deviates considerably from 1, and so in the preceding paper [16], the dependence of the a value on n was regarded as being divided into two straight lines, $a=5.7+0.32n$ for $15\leqq n\leqq18$ and $a=7.3+0.19n$ for $22\leqq n\leqq26$. On the other hand, for the $Im3m$ Cub I phase in the ANBC-14–n-hexadecane system, the a values

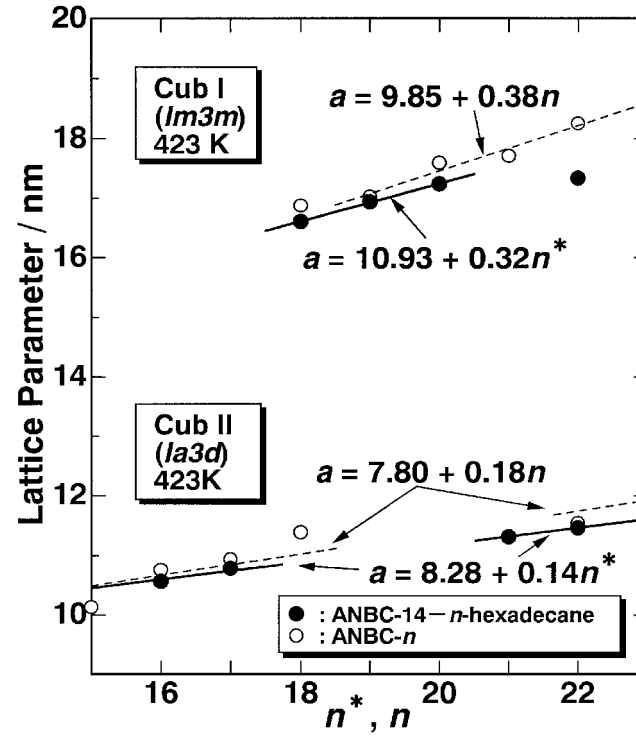

Figure 9. Plots of the cubic lattice constant a versus the effective carbon number n^* for the ANBC-14–n-hexadecane system and versus the alkoxy chain length n for pure one-component ANBC-n. Data plotted are summarized in the table.

Table. Lattice parameter a of the Cub phases of ANBC-n and ANBC-14–n-hexadecane mixtures.

ANBC-n homologues[a]				ANBC-14–n-hexadecane mixtures			
n	Temp/K	Space group	a/nm	n^*	Temp/K	Space group	a/nm
15	465.8	$Ia3d$	10.13				
16	459.2	$Ia3d$	10.76	16.0	423.2	$Ia3d$	10.56
17	453.3	$Ia3d$	10.94	17.1	423.3	$Ia3d$	10.78
18	450.5	$Ia3d$	11.39				
18	458.4	$Im3m$[b]	16.88	18.0	423.3	$Im3m$	16.61
19	429.8	$Im3m$	17.03	19.1	423.2	$Im3m$	16.94
20	433.6	$Im3m$	17.59	20.0	418.4	$Im3m$	17.24
21	423.3	$Im3m$	17.71				
				21.1	423.2	$Ia3d$	11.31
22	428.5	$Im3m$	18.26	22.0	383.8	$Im3m$	17.33
22	456.7	$Ia3d$	11.55	22.0	423.6	$Ia3d$	11.46
26	419.2	$Im3m$	19.74				
26	449.0	$Ia3d$	12.31				

[a] Cited from ref. [16].
[b] Metastable phase [16].

of the first three are on a straight line, satisfactorily fitted by the equation $a = 10.93 + 0.32n^*$ ($r = 0.9995$), but the plot for $n^* = 22.0$ deviates substantially from the dependence of the first three points. For ANBC-n, the a values of the $Im3m$ Cub I phase are well described by the relation $a = 9.85 + 0.38n$ ($r = 0.98$). Compared with the case for ANBC-n, the linearity of the a versus n^* dependence is fairly good for both types of Cub phase (except the $Im3m$ Cub I phase of $n^* = 22.0$) in the ANBC-14–n-hexadecane system. This directly reflects the continuum nature in the aliphatic subspace of the Cub phases in the ANBC-14–n-hexadecane system.

As mentioned in the discussion about figure 7, the presence of two competing molecular parts (aliphatic tail vs aromatic core) is important for the formation of Cub phases, and on increasing the volume fraction of one component, the interfaces that are planar in lamellar structures such as SmA and SmC phases around the fraction 0.5, tend to be deformed with a curvature to result in the bicontinuous Cub phases. In the ANBC-14–n-alkane binary mixture in the present study, an increased amount of n-alkane or increased temperature leads to an increase in the effective volume occupied by the aliphatic component. As for lyotropic $Ia3d$ Cub phases, the $Ia3d$ Cub II structure in ANBC-n, and also that in ANBC-14–n-alkane binary systems, is well described by Luzzati's skeletal graph where the skeletons joined 3-by-3 at both ends form two pairs of networks with cubic symmetry, as shown in figure 10 (b) [7, 15–20]. If one connects the mid points between the nearest skeletons that are not joined, a curved surface, which partitions the Cub space into two equivalent volumes, is obtained and called the G infinite periodic minimal surface (IPMS), an alternative description for the $Ia3d$-type Cub phases. The question arises as to whether the aromatic component lies on the skeletons or on the surface [12], and in figure 10 (b) the former possibility is chosen without any definite evidence. Analysis of the lattice parameters in [16] reveals that *two* dimerized ANBC cores are on a face diagonal line in the unit cell.

On the other hand, bicontinuous $Im3m$ Cub phases are described by two pairs of networks with the skeletons joined 6-by-6 at both ends in Luzzati's graph or by the P-type surface in the IPMS description—for the latter description, see figure 10 (a). From the two plots for ANBC-14–n-hexadecane binary systems shown in figure 9, the ratio of the increment with respect to n^* for the $Im3m$ Cub phase to that for the $Ia3d$ Cub phase is 2.3, and the corresponding ratio is 2.1 for ANBC-n homologues. These values around 2 suggest, as shown in figure 10 (a), that there would be *four* dimerized ANBC cores along the face diagonal line in a unit cell, and thus, if we use the P surface, it should be *doubled* [25]†. Further examination will be reported in a separate paper.

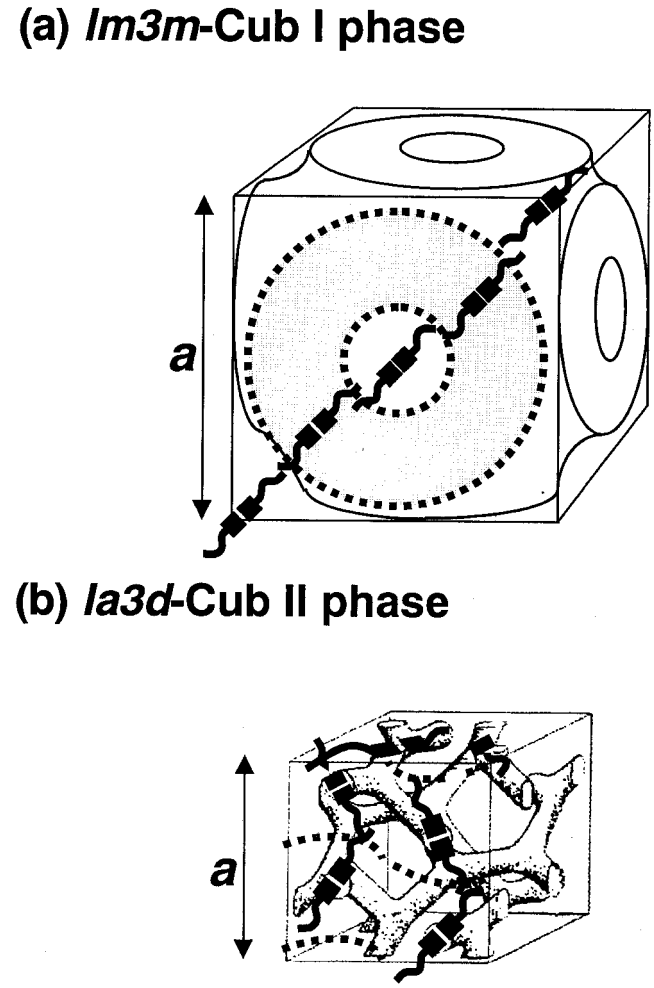

Figure 10. Possible model structure of (a) $Im3m$ Cub I and (b) $Ia3d$ Cub II phases. In (a), the P surface is doubled, and in (b), the dotted curves represent the G surface (see the text).

4. Conclusions

The present studies have established unequivocally the phase diagram in the Cub region for the binary systems ANBC-14 and n-alkane (n-tetradecane or n-hexadecane), where ANBC-14 has an alkoxy chain one carbon atom shorter than the chain length required for the formation of Cub phase(s) in ANBC-n homologues and exhibits *no* Cub phase. The addition of n-alkane to ANBC-14 induces Cub phases, and it was found that the *type* of Cub phases formed is a function of the effective carbon number n^*, instead of the alkoxy chain length n of ANBC-n; the binary system completely reproduces the recently established [16] complicated phase diagram within the Cub region of ANBC-n. This indicates that the formation of the Cub phases and the *phase type* in the one-component ANBC-n can be understood in terms of the presence of two competing parts, hydrophobic and flexible aliphatic tails vs the partly hydrophilic and

rigid ANBC-n aromatic core (containing a hydrogen-bonded COOH linkage), and that the top part of the alkoxy tail really acts as a continuum, as first revealed experimentally by Saito and co-workers by their calorimetric studies [13]. Furthermore, the continuum nature in both the $Im3m$ Cub I and $Ia3d$ Cub II phases has enabled us to depict a possible structure of the $Im3m$ Cub I phase.

We are grateful to Prof. Michio Sorai and Kazuya Saito at Osaka University for the collaborative work on the heat capacity of ANBC-22 and for valuable discussions, and to Prof. Keiichi Moriya at Gifu University for his valuable experimental suggestions. Thanks are also due to Ms Yumiko Murase and Eri Kumita at the Instrumental Analysis Center, Gifu University, for the MS measurements. This work was supported by Grant-in-Aid for Scientific Research on Priority Areas (A), 'Dynamic Control of Strongly Correlated Soft Materials' (No. 413/13031037) from the Ministry of Education, Science, Sports, Culture, and Technology in Japan, and was partly supported by the Research Foundation for Electrotechnology of Chubu (R-11123) and the Saneyoshi Foundation (No. 1343).

Note added in proof

[†]After submitting the manuscript, we learned of this report, which reveals the properties of the 'double' structure of type P.

References

[1] Gray, G. W., and Goodby, J. W., 1984, *Smectic Liquid Crystals* (Glasgow: Leonard Hill), pp. 68–81, including earlier references on thermotropic cubic phases.

[2] Billard, J., Zimmermann, H., Poupko, R., and Luz, Z., 1989, *J. Phys. (Paris)*, **50,** 539, including references on other types of thermotropic cubic phases.

[3] Diele, S., and Göring, P., 1998, *Handbook of Liquid Crystals*, Vol. 2B, edited by D. Demus, J. Goodby, G. W. Gray, H.-W. Spiess, and V. Vill (Weinheim: Wiley-VCH), pp. 887–900.

[4] Gray, G. W., Jones, B., and Marson, F., 1957, *J. chem. Soc.*, 393.

[5] Demus, D., Kunicke, G., Neelsen, J., and Sackmann, H., 1968, *Z. Naturforsch.*, **23a,** 84.

[6] Demus, D., Marzotko, D., Sharma, N. K., and Wiegeleben, A., 1980, *Krist. Tech.*, **15,** 331.

[7] Tardieu, A., and Billard, J., 1976, *J. Phys. (Paris) Coll.*, **37,** C3-79.

[8] Etherington, G., Leadbetter, A. J., Wang, X. J., Gray, G. W., and Tajbakhsh, A., 1986, *Liq. Cryst.*, **1,** 209.

[9] Pelzl, G., and Sackmann, H., 1971, *Symp. chem. Soc., Faraday Div.*, **5,** 68.

[10] Kutsumizu, S., Yamada, M., and Yano, S., 1994, *Liq. Cryst.*, **16,** 1109.

[11] Luzzati, V., and Spegt, P. A., 1967, *Nature*, **215,** 701.

[12] Clerc, M., and Dubois-Violette, E., 1994, *J. Phys. II Fr.*, **4,** 275.

[13] Saito, K., Sato, A., and Sorai, M., 1998, *Liq. Cryst.*, **25,** 525.

[14] Saito, K., Shinhara, T., and Sorai, M., 2000, *Liq. Cryst.*, **27,** 1555.

[15] Kutsumizu, S., Ichikawa, T., Nojima, S., and Yano, S., in Abstracts of ILCC 2000, Sendai, Japan, p. 114.

[16] Kutsumizu, S., Morita, K., Ichikawa, T., Yano, S., Nojima, S., and Yamaguchi, T., *Liq. Cryst.* (submitted).

[17] Levelut, A.-M., and Fang, Y., 1990, *Coll. Phys., Coll.*, **51,** C7-229.

[18] Levelut, A.-M., and Clerc, M., 1998, *Liq. Cryst.*, **24,** 105.

[19] Kutsumizu, S., Ichikawa, T., Nojima, S., and Yano, S., 1999, *Chem. Commun.*, 1181.

[20] Kutsumizu, S., Ichikawa, T., Yamada, M., Nojima, S., and Yano, S., 2000, *J. phys. Chem. B*, **44,** 10 196.

[21] Gray, G. W., Hartley, J. B., and Jones, B., 1955, *J. chem. Soc.*, 1412.

[22] Kutsumizu, S., Yamaguchi, T., Kato, R., and Yano, S., 1999, *Liq. Cryst.*, **26,** 567.

[23] Rançon, Y., and Charvolin, J., 1988, *J. phys. Chem.*, **92,** 2646.

[24] Imperor-Clerc, M., Sotta, P., and Veber, M., 2000, *Liq. Cryst.*, **27,** 1001.

[25] Schwarz, U. S., and Gompper, G., 1999, *Phys. Rev. E*, **59,** 5528.